Proceedings World Geothermal Congress 2020+1
Reykjavik, Iceland, April - October 2021

Multiscale and Multimethod Investigation on Outcropping Analogs: Key Tool for Resources Evaluation and Predrilling Modelling for Geothermal Prospection in Extensional Faults

Lionel Bertrand[1], Claire Bossennec[1], Le Maire Pauline[2], Dupont Benjamin[2], Yves Géraud[1] and Marc Diraison[1]

[1]Université de Lorraine, GeoRessources, F- 54000 Nancy, France

[2]Université de Strasbourg/EOST, CNRS, Institut de Physique du Globe de Strasbourg (IPGS UMR 7516), Strasbourg, France

Lionel.bertrand@univ-lorraine.fr, claire.bossennec@univ-lorraine.fr, pauline.lemaire@unistra.fr, benjamin.dupont2@etu.unistra.fr, yves.geraud@univ-lorraine.fr, marc.diraison@univ-lorraine.fr

Keywords: multimethod geophysics, fractured basement rocks, fault zone architecture.

ABSTRACT

The grabens related to the West European Rift system are targets of several drilling projects for geothermal high temperature prospection. Due to the low thermal gradient in comparison to the geothermal fields located in volcanic or active rift areas, the targeted reservoirs are located at great depth, in the fault zones in the metamorphic or magmatic basement rocks. Unfortunately, the reservoir properties and structural knowledge necessary for resources evaluation, predrilling modelling and borehole design are poorly investigated, due to lack of existing boreholes and seismic data with a suitable resolution at great depth. In this context, the DONUTS project, financed by the GIS Géodénergies aims to develop an integrated method for the geothermal prospection, by combination of Geological and high-resolution geophysical data on outcrop analogs, and large-scale geophysical investigation in the graben (seismic, aeromagnetic, gravimetric et magnetotelluric data).

In this study, we show the first tests on outcropping fault zones in the Limagne and the Upper Rhine Graben shoulders. It consists on the development of a new methodology of fractures characterization on 3D data acquired with Lidar or UAV photogrammetric models. On this first step, the comparison between the 3D model and the fracture characterization on the outcrop offers promising results for the development of the method. High resolution geophysical prospection are tested on outcropping fault zone and basement/sedimentary interfaces, with examples on new methodology of aeromagnetic multi-altitude mapping with UAV, resistivity and seismic profiles. They show preliminary results in fault zone detection that will be later enhanced by comparison and modelling of the linked physical properties measured on rock samples. After that, there will be a work on upscaling the fault zones properties and geophysical results in order to constrain the large-scale data.

1. INTRODUCTION

The grabens related to the West European Rift system are targets of several drilling projects for geothermal high temperature prospection. Due to the low thermal gradient in comparison to the geothermal fields located in volcanic or active rift areas, the targeted reservoirs are located at great depth, in the fault zones in the metamorphic or magmatic basement rocks or at the immediate sedimentary coverage. Due to the depth and rock types, the geothermal prospection suffers from two main scientific problems. The target prospection is exposed to a global lack of data: few or none existing boreholes for host rock and reservoir properties characterization and difficulty to map the reservoir geometry with the subsurface geophysical acquisition (Bertini et al., 2006; Luthi, 2005).

The reservoir properties of the targeted fault zones are related to the fractured network linked to the regional and local tectonic history and the alteration process du to fluid flows, ancient or actual (Nelson, 2001). These processes are unfortunately not accessed before the first drilling for resource estimation and associated business-model building. To offset this lack of data, a classical methodology is to use outcropping analog rocks of the targeted buried formation and perform laboratory experiments for petrophysical properties estimation and fields studies for fracture network characterization (McCaffrey et al., 2003). However, the applicability for modelling the buried reservoir properties from outcrop measurements raises difficulties for evaluate their variation du to the difference in burial history, surface weathering process, etc. For the fracture network, the link between fractures measurements on outcrop as scan lines or fracture maps, and also the boreholes fracture imagery, regarding to the real buried fracture network in 3D is also difficult to establish for a precise fluid flow modeling. The fracture network are therefore mostly modelled with equivalent porosity and permeability models, or in better cases with statically equivalent parameters of length, density, … (La Pointe et al., 2002; Davy et al., 2006; Sausse et al., 2010; Bisdom et al., 2014). In such models, reservoir and also fracture network properties on outcrop suffers of hard hypothesis that the comparison to the results during drilling exploration, diagraphs or flow measurements, is often resumed to qualitative considerations (Luthi, 2005; Cuong and Warren, 2009; Vidal et al., 2017).

Before resources estimation, the geothermal exploration has to locate the fault zones in the basement, with significant throw, thickness, and associated secondary structures in order to allow enough natural hot fluid flow. In continental basin context, a classic way is to use seismic prospection, eventually helped with gravimetric and aeromagnetic data that estimate the basement/sedimentary interface thickness and basement rock lithology (Edel et Schulmann, 2009). However, the fault network models in the basement are often reduced to prolongation of the faults detected in the immediate sedimentary cover, and basement topography as “loss of sedimentary horizons signal” on the seismic lines (Khair et al., 2015; Carpentier et al., 2016). The secondary fault network or damaged zone and highly altered fault cores thickness hosting the fluids flows are never reachable in these prospects. The basement lithology, first order parameter for reservoir modelling, is often only qualitatively linked the gravimetric or aeromagnetic anomalies, without precise geological or rock properties constrains (Edel et Schulmann, 2009; Edel et al., 2018).

The DONUTS project funded by the GIS Géodénergies is devoted to enhance the translate process between outcropping rocks data and subsurface geophysical data for geothermal prospection. The goal of the project is to propose a set of geophysical and modelling solutions for the detection and estimation of the reservoir properties of faulted rocks in buried basement lithologies. It relates to an iteration process from classical geological characterization on outcroping fault zones, link the petrographic and petrophysical properties with high resolution geophysical prospection on the outcrop, and finally upscale the results to subsurface scale prospection for geothermal reservoirs. As the project is at the beginning, this paper introduces the first clues and ideas of development on outcropping examples for better constraining the fracture network on outcrop analogs, and tests of high-resolution geophysical prospection on fault zones and basement/sedimentary interface. They consist on an example of fault zone compartmentalization with a new methodology of multi-altitude UAV aeromagnetic cartography, and resistivity and seismic profiles on outcropping areas.

2. GEOLOGICAL BACKGROUND

The areas of interest are related to the West European Rift (WER) grabens and their shoulders where the basement rock outcrops, with a focus on the Northern Vosges (V) as outcropping basement of the Upper Rhine Graben (URG) and the Massif Central at the shoulders of the Limagne Graben (LG) (Figure 1).

The basement rocks are originally emplaced during the Hercynian orogeny between 360 and 300 Ma. It is composed of different lithotectonic domains that are related to the plate tectonics before the final collision between Gondwana at the South and Laurentia and Baltica at the North, with several microcontinents like Armorica or Avalonia stuck between them (Matte, 2001; Nance et al., 2010; Guy et al., 2011; Lardeaux et al., 2014). In the Muckenbach area, the basement rocks are composed of the volcano-sedimentary low-grade metamorphic Bruche unit, a devonian basin that belongs to the Saxothuringian domain (Skrzypek et al., 2014), and Carboniferous granites and diorites emplaced during the extension linked to the orogenic collapse (Tabaud et al., 2014). These granites are also the basement of the Cleebourg Triassic sandstones and the Saint-Pierre-Bois Pennsylvanien sediments. In the Limagne areas, the outcrop used is located in the so called “Tufs-antracifères series”, that is a Late-Visean undeformed volcano-sedimentary unit that belongs to the Moldanubian domain (Faure et al., 2002, 2009).

After the orogenic collapse begins a period of extension in this part of Europe that starts from Pennsylvanian in very small basins and progressively enlarges until the Jurassic Period (Guillocheau et al., 2000; Sissingh, 2001; Bourquin et al., 2006). It is followed by the opening of the North Atlantic Ocean during the Cretaceous Period and the collision between the African and European plates, both leading to a reactivation of the inherited structures (Srivastava et al., 1990; Olivet, 1996). In response to the collision, the WER starts at the end of the Eocene Epoch and led to the formation of several N-S grabens (Roussé, 2006; Bourgeois et al., 2007; Edel et al., 2007; Ford et al., 2007) (Figure 1). The maximum extension rate was reached in thee Oligocene Epoch, followed by the Transtensionnal regime in the Miocene due to a rotation of the regional stress.

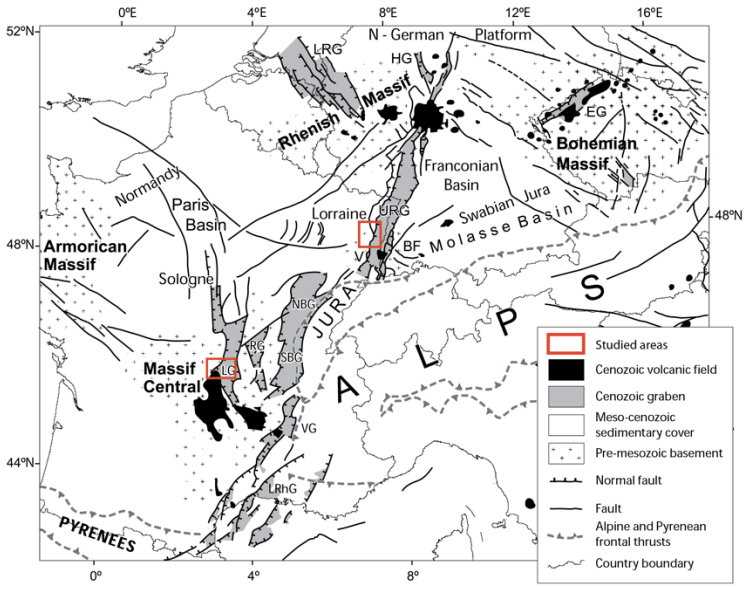

Figure 1: General map of the WER grabens and outcroping pre-mesozoic basement with the two areas of interest of the study, modified after Bourgeois et al. (2007).

3. FAULT ZONE ARCHITECTURE AND PETROPHYSICAL PROPERRTIES

The fault zones (FZ) are classically described in three parts with 1) a fault core (FC), where the main brittle deformation is located. It can be composed of a single slip plane, breccias and highly altered material or a clay-rich and non-cohesive gouge or also hard cataclasis. 2) The damaged zones (DZ) surrounds the FC and is defined as a fractured areas with a fracture density higher than 3) the undeformed protolith rock (Faulkner et al., 2010). This fracture density is classically described with an exponential function linked to the distance to the FC (Mitchell and Faulkner, 2012). In function of the nature and proportion of the different FZ parts, the FC and DZ can both act as conduit or barrier for the fluid flow (Caine et al., 1996). This induces high anisotropies of the flow properties along and through the FZ, and many configuration possibilities that also varies along the fault surface. A general

classification can however be made of the fault zone properties in function of the rock lithologies, depending mainly of their clays content and their hardness (Bense et al., 2013).

In silicoclastic sedimentary rocks, the presence of clays horizons will favor the development of less permeable FC due to clay smearing, and the presence of sandy horizons can have both effect on the permeability depending of the degree of cataclasis (Bense and Person, 2006; Loveless et al., 2011) (Figure 2a & b). It will also create a high permeability anisotropy between fault plane and perpendicular to fault direction. In the crystalline rocks, the contrast between the clay rich (by smearing or precipitation linked to fluids) FC and the DZ often highly fractured led to a high contrast of permeability between FC and DZ but not a very high anisotropies in direction (Chester and Logan, 1986 ; Forster and Evans, 1991) (Figure 2c). In volcanic rocks, the lithology properties of the protolith is often very variable, FZ having one or the other properties described above, or even a mix between them (Wilson et al., 2003; Gray et al., 2005; Riley et al., 2010; Walker et al., 2013). In carbonates, dissolution process linked to fluid flow led often to the development of permeable cavities in the FC, when it is not plugged by clays (Ferrill and Morris, 2003; Agosta et al., 2007; Agosta, 2008) (Figure 2d).

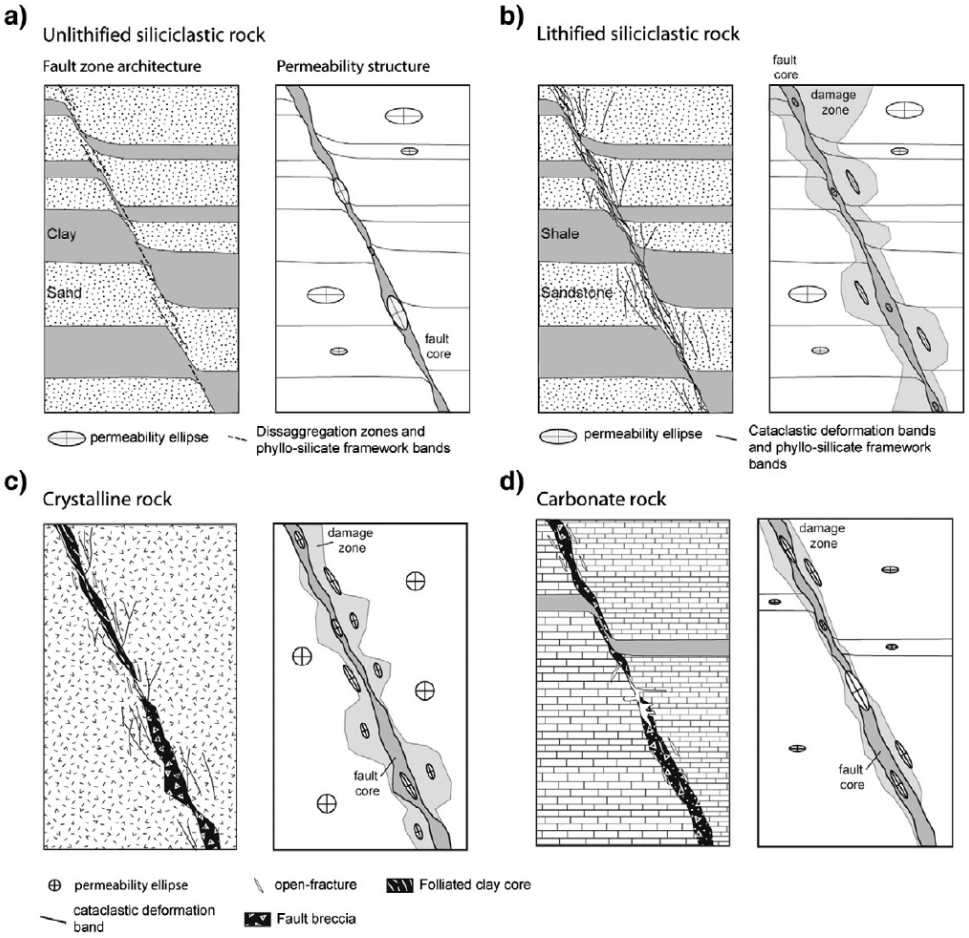

Figure 2: Damaged zone and fault core structure and associated permeability ellipse classified by protolith lithology after Bense et al. (2013).

The definition of the FZ architecture depends also of the scale of the study. Thus, a fault on a satellite view or a seismic profile will be a single fault trace (Figure 3a). When studied at higher resolution, this single trace can be divided as the FZ model described before with one or several FC and DZ parts (Figure 3b & c). It has also been shown that there is often secondary FC in the DZ parts (Le Garzic, 2010). These can be described by their own FC/DZ architecture that is visible in a higher resolution scale, and so on until the microscopic scale (Figure 3d & c).

Thus, the characterization of the FZ architecture and the linked petrophysical properties is a key objective for predicting the fluid flows. Many studies are focalized in the analysis of FZ throw, thickness or length. These lead to the definition of statistical laws that link these parameters and help to estimate for example the DZ thickness from the throw detected on seismics (Kim et Sanderson, 2005; Childs et al., 2009; Faulkner et al., 2011). The fractured network linked to the FZ is also widely studied in different areas and geological contexts. These studies have mainly a statistical approach on fracture parameters like length, density or spatial distribution, with the aim to describe the most completely possible the fracture network in the DZ (Bonnet et al., 2001; Nelson, 2001; Berg et Øian, 2007). In general, the representativity of the results acquired by 1D (with scan lines on the outcrop or boreholes imagery) or 2D (satellite image or geological map and seismic study) and the real fracture network in 3D are not fully documented or controlled. Several statistic laws exist to convert the data in 3D with their advantages and assumptions (Bourbiaux et al., 1998; Bour et Davy, 1999; Bonnet et al., 2001; Wang, 2005). A main question of these laws is depending on the scale of the model, i.e. which fracture size can be considered as “matrix” in the rock mass in opposition to those who have size enough to be modeled as independent surface of flow.

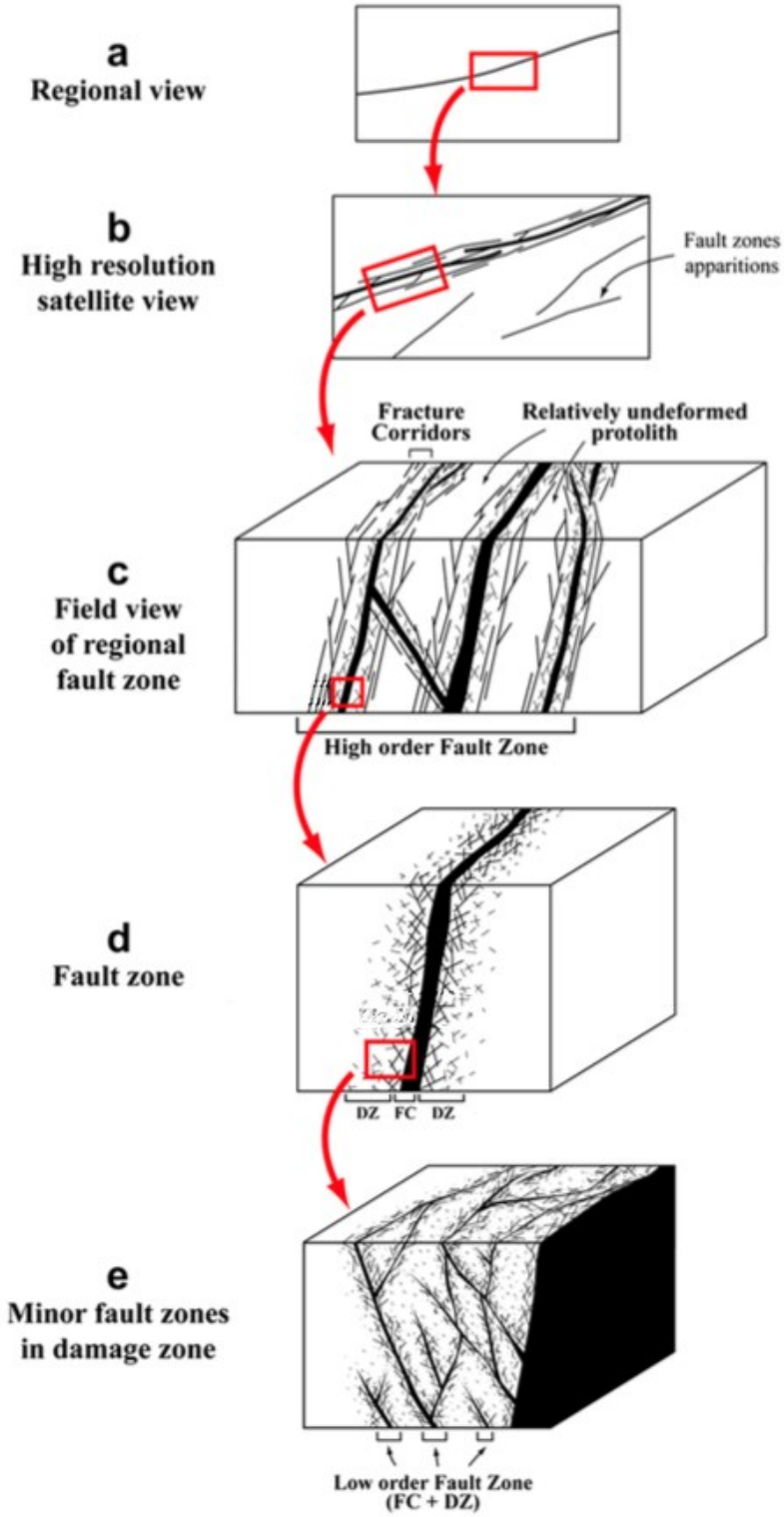

Figure 3 : Schematic fault zone architecture observed at different scale from the regional view to the outcrop scale (Le Garzic, 2010).

At the opposite, the petrophysical properties in terms of rock matrix, i.e. mineralogical and fractures under the resolution of the statistical properties is not systematically studied, in particular for rock classically considered as “low matrix porosity” as granites or metamorphic rocks. This statement has been widely addressed by many studies that considers ranges of variations of porosity (Mielke et al., 2017 Kushnir et al., 2018). These studies consider globally only fresh samples and addresses the variability of the properties with the mineralogy in the protolith. How these properties vary in FZ regarding the alteration degree and the fracture intensity remains a question unresolved in many prospects. One reason of this lake of information is the very few sites where properties measured on diagraphs (i.e. resistivity, porosity logs,…) are compared to petrophysical measures on cores or analogs rocks. Porosity and permeability of FZ are thus mostly derived from hydraulic test after drillings and demonstrate the variability of the FZ properties, with permeabilities going from 0.02 to 1000 mD (Bächler et al., 2003; Stober et Bucher, 2007; Baujard et al., 2016; Bucher et Stober, 2016).

4. PRELIMINARY RESULTS:

To get a better pre-drilling estimation of the rock properties in the basement rocks and the immediate sedimentary cover of the grabens linked to the WER, the DONUTS project focusses on FZ on rock analogs at the outcrop on the rift shoulders. Rock matrice properties evolution in FC and DZ was already performed (Bertrand et al., submitted) and the fracture network studied on the URG (Bertrand et al., 2018). The objectives are now to better constrain the geophysical investigation regarding matrice and fractures, with a first step on high resolution geophysical prospection on outcrop, before upscaling the result at the scale of industrial prospection. The results presented are thus first clues and objectives that will be enhanced during the project. It is firstly a methodology development for fracture network analysis on 3D data from Lidar or UAV photogrammetry for better constrain the SL representativity with an outcrop on the Limagne shoulders. Then we show first tests of geophysical prospection on FZ in the Vosges Mountains, with multi-altitude drone UAV aeromagnetic measurements and fault mapping, resistivity profiles on an outcropping basement/sedimentary interface and finally seismics on a FZ in Triassic sandstones.

4.1 Fracture network characterization.

Fracture networks are widely studied with 1D scan lines or boreholes or 2D maps that aims to statistically reflect the network in 3D, with conversion laws between the different dimensions tested on synthetic cases (Bourbiaux et al., 1998; Bour et Davy, 1999; Bonnet et al., 2001; Wang, 2005). To test this conversion and to go further in upscaling the fracture properties from metric to decametric length on quarries and cliffs, we develop a new methodology of fracture characterization. With photogrammetric data from UAV survey or Lidar data, the outcrop is reconstructed in 3D and the fracture planes are modelld by Cloudcompare® plug-in FACETS® and ArcGIS software®. The first one led to a detection of plane surfaces with their orientation (Dewes et al., 2006) and the second is used for reconstructing the fracture plane by combination of the adjacent surfaces with the same orientation. The plug-in has already successfully been tested for fracture orientation on andesitic lava flows (Massiot et al., 2017), but the fractures reconstitution shows in addition length/surface data and density.

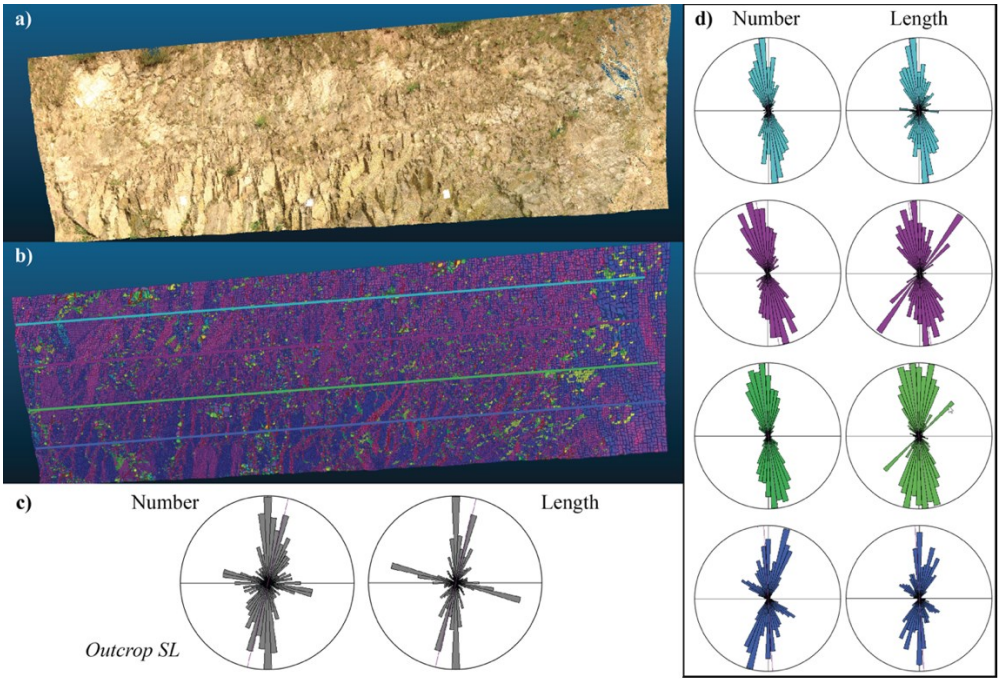

Figure 4: a) 3D reconstitution of the fractured basement in the Limagne area from Lidar data points, b) plane reconstitution using FACETS plug in on Cloudcompare, colors indicating the variation of plane orientation, c) fractures orientation measured on the field by scan line method (bleu line), d) fractures orientation on the four synthetic scan lines on the 3D model.

The first test has been performed on Lidar data on the Limagne shoulders on visean metamorphic rocks. Figure 4a shows the raw data from the Lidar acquisition and figure 4b the surface detection with FACETS before fracture plane reconstitution. On this model, four synthethic scan line were drawn and the results in orientation compared to SL performed on the outcrop (Figure 4c). On the outcrop, four main fractures families can be distinguished in number and also in length: N-S, NNE-SSW ESE-WNW, and a minor one NNW-SSE. The synthetic SL on the same spatial location on the model is shown in blue. Similar four fractures direction are highlighted, even if the ESE-WNW is slightly switched to a more NW-SE direction. In numbers, the NNE-SSW is the main fracture set, but it is corrected by weighting by the fracture surfaces. This is due to the outcrop surface direction that statistically surexpose the NE-SW direction in number of detected fracture planes compared to the orthogonal direction of the outcrop, and that is corrected by the surface weighting. This comparison between the modeled outcrop and the field data offers therefore promising results for fracture network reconstruction in 3D where it is not possible to directly asses the outcrop, or for fracture length too large to be by hand characterized.

Another concluding remark on this first test is the representativity of a SL on outcrops regarding the whole fractured system. Assuming the validity of the fracture planes reconstitution from the comparison between SL on the outcrop and on the model, other synthethic SLs are drawn on higher parts of the outcrop (colored lines, figure 4b). As main fracture direction is always around the N-S direction, the general fracture pattern is different on each SL : NE-SW fractures are not detected on the outcrop SL but are

present on the green and purple SLs, and the more scattered diagram signal does not allow the distinction between the N-S and NNE-SSW fractures. At the summit of the outcrop, the main trend is N-S and the other fractures directions are not represented. This variation highlights the spatial variability of the fracture network in this kind of lithology and geological context. It shows therefore that such characterization on outcrop should be used with caution and invite to a multiplication of SLs location for a better representativeness of the results.

4.2 Multi-altitude aeromagnetic survey

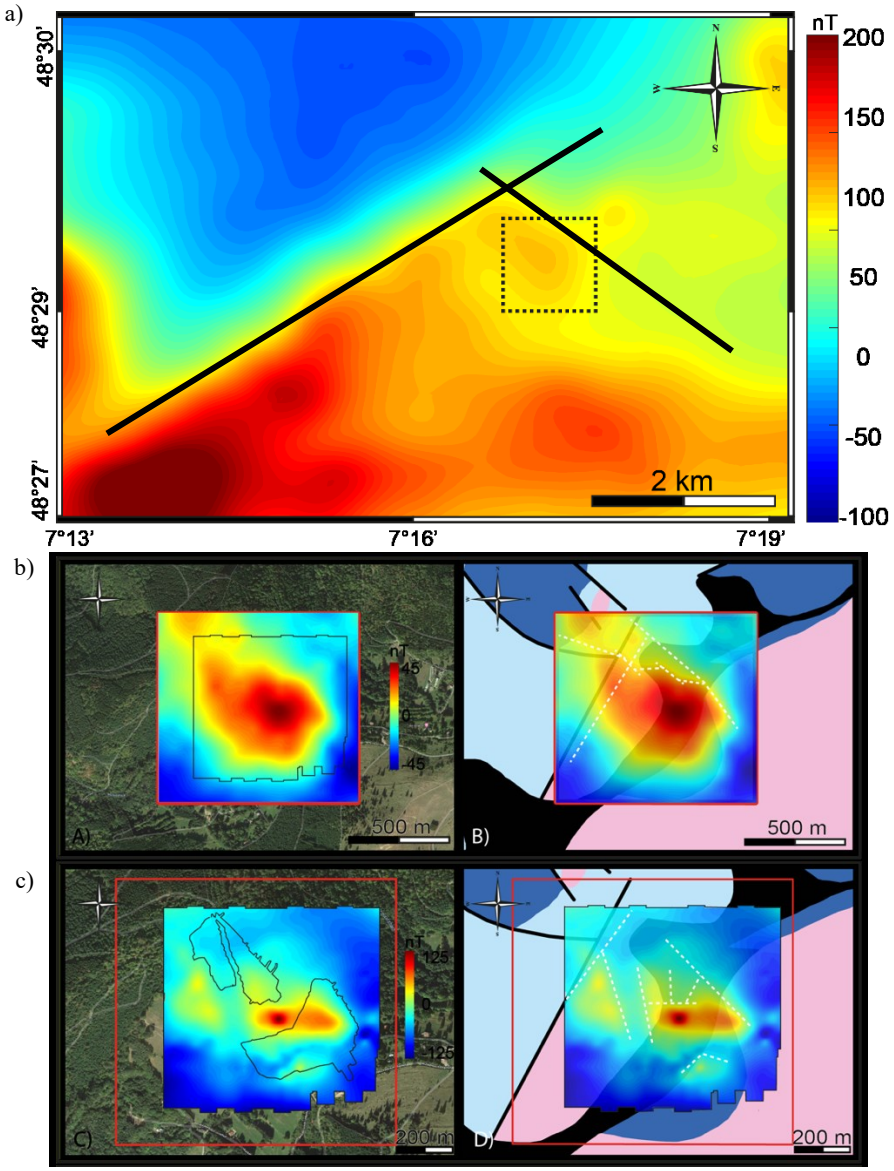

Figure 5: a) TMI of Helicopter aeromagnetic survey at 400m altitude above ground level (AGL) in the Northern Vosges. (modified after Bertrand et al. (in revision)), the dotted square is the Muckenbach area; Drone aeromagnetic survey, b) at 100 m AGL and c) at 30 m AGL, TMI at the left and interpretation above the geological map at the right (modified after Le Maire et al. (accepted)). The blue is the Bruche volcano-sedimentary unit, pink is the Carboniferous granite and in black is the diorite.

In the URG, regional aeromagnetic surveys have been done in order to constrain the deep structures of the graben related to the outcropping areas in the Vosges and Black Forest mountains (Edel et Schulmann, 2009). In the Northern Vosges, the scale effect on magnetic anomalies linked to regional faults has been tested with a new methodology with drone surveys at different altitudes in the Muckenbach area (Le Maire et al., accepted). A first order NE-SW fault marks in the studied area the contact between the Carboniferous Granites in the Southern part and Metamorphic units at the North (Figure 5a). This fault is hidden at the surface by the smooth contact between the granites and the metamorphic rocks (Bertrand et al., in revision). A secondary anomaly shows also a NW-SE fault in the granites, a direction that is also documented in other part of the Northern Vosges (Bertrand et al., 2018). The drone surveys at different altitudes (100 and 30 m) are managed on this secondary fault. They show the progressive compartmentalization of the anomaly as the flight comes closer to the ground, i.e. the magnetic anomalies are more precise and linked to less deeper objects. Thus, the anomaly corresponding to the NW-SE fault trace on the geological map is divided in E-W and SW-SE hectometric sections in the 100 m drone flight (Figure 5b). On the 30 m flight, the NE-SW signature is smoothed and almost disappear in aid of N-S structure in an anomaly with a E-W trend (Figure 5c).

Thus, this multi-altitude surveys shows the compartmentalization of the fault network with the scale. As showed in figure 3, the regional scale NW-SE fault is subdivided in a combination of N-S and ESE-WNW on a higher resolution. Further work will be to use the multi-altitude survey and the magnetic susceptibilities measured on rock samples of the areas in order to better constrain the geometry and the in depth investigation.

4.3 Resistivity on basement/sedimentary interface

Resistivity profiles are often used to detect fluid flows, mainly in volcanic areas where the presence of flow and clays-rich cap rock can be mapped in depth (Cumming and Mackie, 2007, 2010). It can also be used to detect the basement rock interface du to large change in matrice porosity between the two formations. This was tested for the URG context in the Saint-Pierre-Bois Quarry, where hercynian granite is covered by Pennsylvanian sandstones (Figure 6a). The basement/sedimentary unconformity is localy displaced by normal faults with few meters throw. Several resistivity profiles were performed at the summit of the Quarry in order to test the detection of this interface and these faults. Figure 6b shows an example of resulting resistivity pseudosection with a Dipole-Dipole configuration.

As the contrast of the resistivity in the granite are not yet fully understood, the basement – sedimentary uniformity is well marked on the resistivity pseudosection (Figure 6b). Sedimentary facies are here low resistivity (< 500 Ohm.m) contrasting with the one or two orders of magnitude more resistive granite. The thickness of the less resistive layer corresponds well to the thickness of the sediments above the Quarry. The interface is shifted at two places that corresponds cartographically on normal fault (Figure 6b). However, their propagation in the granite is not clearly constrained by the resistivity survey. The next step of the work will be to better constrain the resistivity properties in the sedimentary cover and also their variation with the alteration of the granite. It will also consist on the modelling on synthetic fractured granite in order to test the influence of the resistivity propereties.

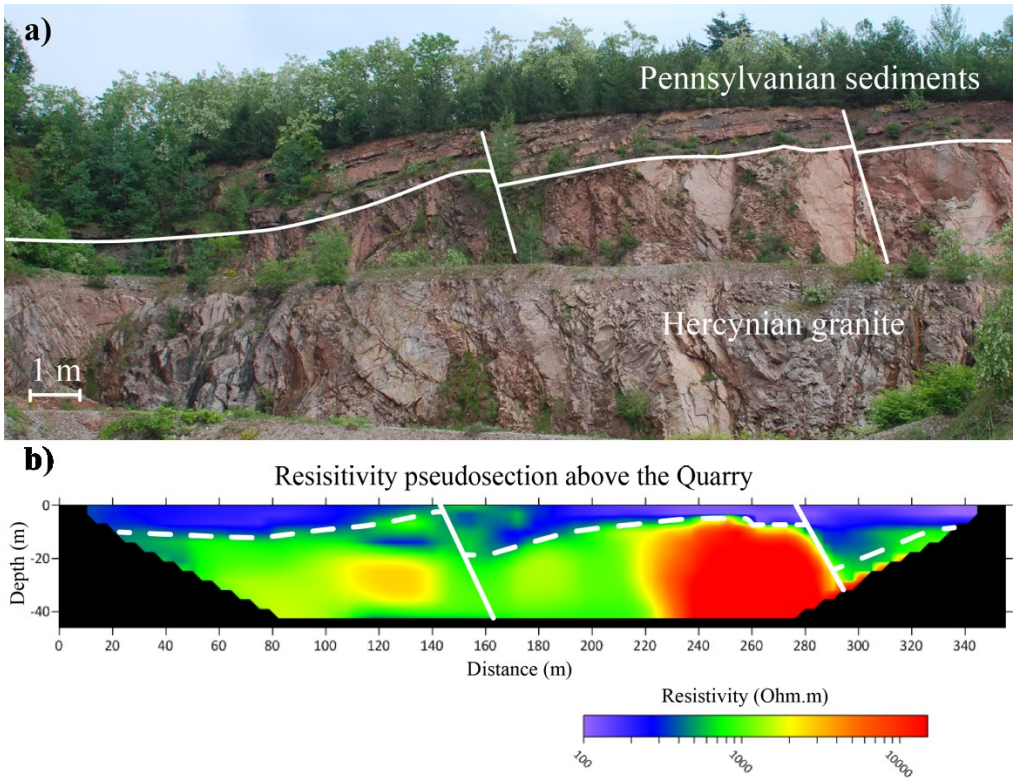

Figure 6 : a) View of the Saint-Pierre-Bois Quarry with hercynian granite covered by Pennsylvanian sandstones with and exemple of small normal faults, b) resisitivity pseudosection derived from Dipole-dipole investigation at the top of the Quarry.

4.4 Seismic profiles in Triassic sandstones

On the Cleebourg Quarry, a fault zone in the Triassic sediments is overlying the basement rocks of the URG. The fault zone is composed of multiple slip surfaces, deformation bands and fractures, isolating less deformed host-rock lenses. Clay-smearing surfaces were also identified in the fault-core (Bauer et al., 2015). The damaged zone is characterized by brittle deformation, and the hanging wall is outcropping on over 50 meters (Figure 7a). The footwall damage zone is not outcropping. Previous studies (Bauer et al., 2015; Bossennec et al., 2018) of the fracture network have shown that the DZ is identified at the outcrop scale by 3 fractured corridors, in which fracture intensity is superior to 4 fractures per meter. Outside of these corridors, the fracture intensity is lower, with mostly fault synthetic fractures, striking NNE-SSW and diping ESE. The thickness of the fracture corridors is averaging 5m, and the distance between these corridors is increasing with the distance to the fault core. The 3 high fracture intensity corridors are identified also on the crack intensity profile measured on thin sections from samples collected in the damage zone.

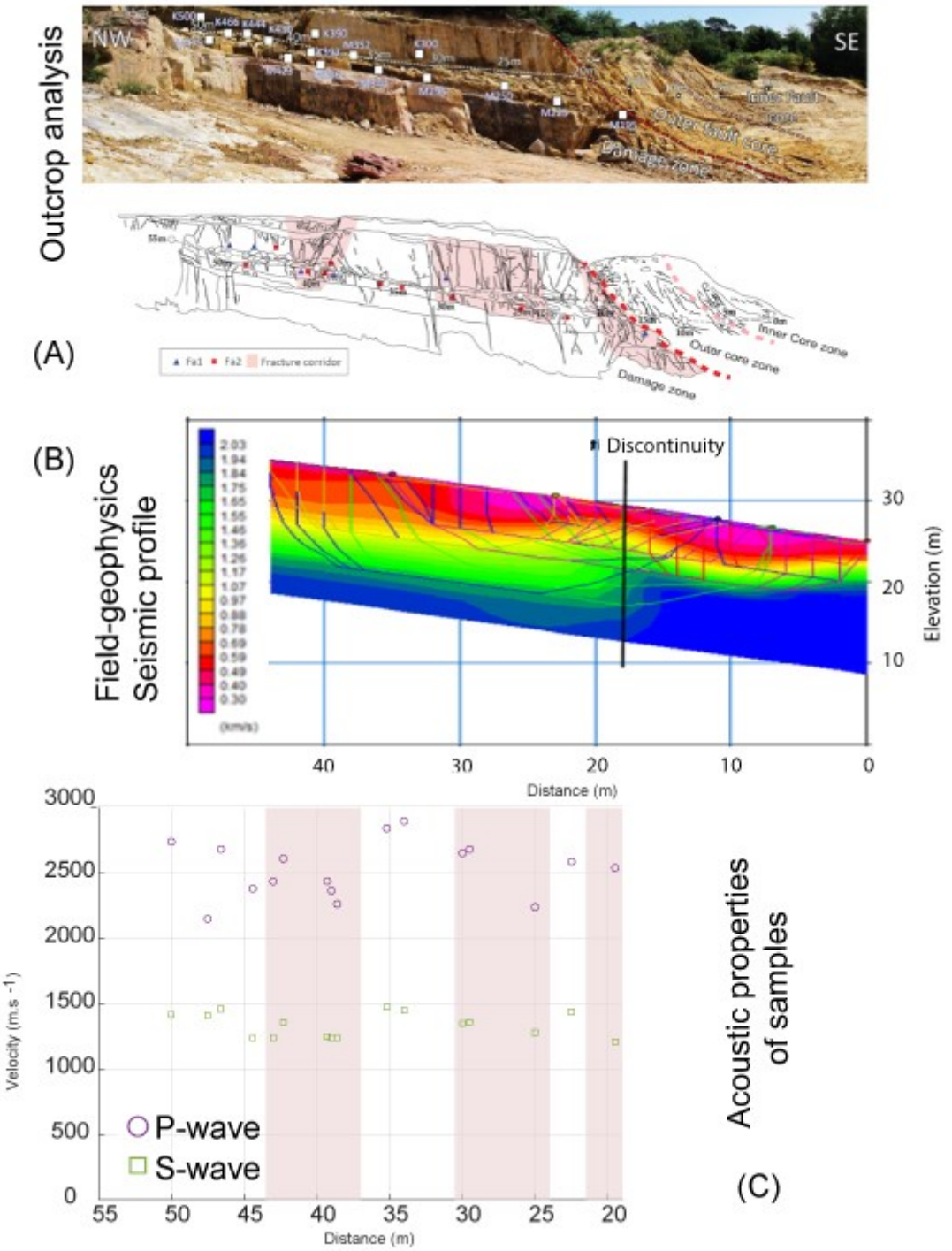

Figure 7: Multi-scale analysis of acoustic properties in faulted sandstones, Cleebourg Quarry. (A) Panorama from the north face of the quarry, with sampling and interpreted tectonic structures, with fracture corridors identified in the fault damage zone (Bossennec et al., 2018) (B) Seismic profile measured on the top of the quarry face to image underlaying structures. (C) Profile of P-and S-waves measurements obtained on samples from the damage zone (Bossennec et al., 2018). The values measured on sample scale are not identical to the bulk values issued from field-seismic profile.

The P- and S-waves values were used to determine dynamic mechanical properties of the sandstones within the damage zone. E (Young's Modulus) is raging from 5.36 to 9.29 GPa, with the lowest values in highly fractured areas, and with a global increase of E with distance to the fault core. Poisson's ratio are relatively similar, and stays constant (average 0.3).

A seismic profile was performed on the top of the quarry face to the image underlaying structures. The image is resulting from a 2 layers modelling of the velocity of the seismic profile. The damage zone observed on the outcrop is identified on the seismic profile by a discontinuity between two domain showing a variable gradient of velocity with depth on each side of the border between the fault-core and the fault damage zone (Figure 7c). The P-waves values on the seismic profile range from 300 to 2000 m/s, whereas P-waves velocity values on samples are comprised between 2100 and 2800 m/s, and S-waves, between 1300 and 1500 m/s

(Bossennec et al., 2018). The comparison of these measurement profiles at different scales underlines the variability of the ranges of values between the profile at the hectometric scale and the values obtained on samples in the laboratory. The transition from one scale to the other is complicated by the presence of tectonic structures that influence the acoustic properties in a variable way, which will focused in the further work.

CONCLUSIONS

This paper shows the scientific philosophy and the first tests of the DONUTS project. The global goal is to enhance the link between geological data and predrilling resource estimation on fault zones targeted by several drillings' projects for high temperature geothermal purpose. It will be an iterative work between obtaining the petrophysical and fracture properties of fault zones at the outcrop, high resolution geophysical investigation and modeling of these objects and finally upscaling the results at the basin scale with the industrial geological prospections. The first clues presented is in the fracture characterization process, with a development of fracture plane reconstitution in 3D with Lidar or UAV photogrammetric data, that will led to a better representativeness of the measurement fracture parameters and allow to sample metric to hectometric fractures. In the second step, the first tests on aeromagnetic mapping, resistivity and seismic profiles shows promising results in fault zone and basement/sedimentary cover detection. The next part of the work will be to use Vp & Vs, electric resistivity and magnetic susceptibility on rock samples that will be linked to the reservoir properties variation to better constrain these geophysical investigations regarding the fault zones architectures. Combined to new numerical solution developments, the upscaling of the results will bring new constrains and prospecting guidelines for industrial geophysical prospection, for example with the detection of the fracture density with seismic data of rock alteration in aeromagnetic or resistivity surveys.

REFERENCES

Agosta, F., Prasad, M., Aydin, A.: Physical properties of carbonate fault rocks, Fucino basin (Central Italy): implications for fault seal in platform carbonates. *Geofluids*, **7**, (2007), 19–32.

Agosta, F.: Fluid flow properties of basin-bounding normal faults in platform carbonates, Fucino Basin, central Italy. *Geological Society of London Special Publication*, **299**, (2008), 277–291.

Bächler, D., Kohl, T., Rybach, L.: Impact of graben-parallel faults on hydrothermal convection – Rhine Graben case study. *Physics and Chemistry of the Earth*, **28**, (2015), 431–441.

Bauer, J.F., Meier, S., Philipp, S.L.: Architecture, fracture system, mechanical properties and permeability structure of a fault zone in Lower Triassic sandstone, Upper Rhine Graben. *Tectonophysics,* **647–648**, (2015), 132–145.

Baujard, C., Genter, A., Dalmais, E., Maurer, V., Hehn, R., Rosillette:Temperature and hydraulic properties of the Rittershoffen EGS reservoir, France. *Proceedings*, European Geothermal Congress, Strasbourg, France, 19-24 Septembre, 1-8 (2016).

Bense, V.F., Person, M.: Faults as conduit-barrier systems to fluid flow in siliciclastic sedimentary aquifers. *Water Resources Research*, **42**, (2006), W0542.

Bense, V.F., Gleeson, T., Loveless, S.E., Bour, O., Scibek, J.: Fault zone hydrogeology. *Earth-Science Reviews*, **127**, (2013), 171-192.

Berg, S.S., Øian, E.: Hierarchical approach for simulating fluid flow in normal fault zones. Petroleum Geoscience, **13**, (2007), 25-35.

Bertini, G., Casini, M., Gianelli, G., Pandeli, E. : Geological structure of a long- living geothermal system, Larderello, Italy. *Terra Nova*, **18**, (2006), 163–169.

Bertrand, L., Jussaume, J., Géraud, Y., Diraison, M., Damy, P.C., Navelot, V., Haffen S.: Structural heritage, reactivation and distribution of fault and fracture network in a rifting context: Case study of the western shoulder of the Upper Rhine Graben. *Journal of Structural Geology*, **108**, (2018), 243-255.

Bertrand, L., Gavazi, B., Mercier de Lépinay, J., Diraison, M., Géraud, Y., Munschy, M.: On the use of aeromagnetism for geological interpretation part II: geological interpretation on outcropping basement rocks as analogs for geothermal prospects. *Journal of Geophysical Research, solid earth*, in revision.

Bertrand, L., Diraison, M., Géraud, Y.: Petrophysical properties of faulted basement rocks: insight from outcropping analogues on the West European Rift shoulders. *Submitted to Geothermics*.

Bisdom, K., Gauthier, B.D.M., Bertotti, G., Hardebol, N.J.: Calibrating discrete fracture-network models with a carbonate three-dimensional outcrop fracture network: Implications for naturally fractured reservoir modeling. *American Association of Petroleum Geologists Bulletin*, **98**, (2014), 1351-1376.

Bonnet, E., Bour, O., Odling, N.E., Davy, P., Main, I., Cowie, P., Berkowitz, B.: Scaling of fracture systems in geological media. *Reviews of Geophysics*, **39**, (2001), 347383.

Bour, O., Davy, P.: Clustering and size distributions of fault patterns : theory and measurements. *Geophysical Research Letters*, 26, (1999), 2001-2004.

Bourbiaux, B., Cacas, M.-C., Sarda,S., Sabathier, J.-C. : A rapid and efficient methodology to convert fractured rservoir images into a dual-porosity model. *Revue de l'institut Français du Pétrole*, **53**, (1988), 785-799.

Bourgeois, O., Ford, M., Diraison, M., Le Carlier de Veslud, C., Gerbault, M., Pik, R., Ruby, N., Bonnet, S.: Separation of rifting lithospheric folding signatures in the NW Alpine foreland. *International Journal of Earth Sciences*, **96**, (2007), 1003-1031.

Bourquin, S., Peron, S., Durand, M.: Lower Triassic sequence stratigraphy of the western part of the Germanic Basin (west of Black Forest): Fluvial system evolution through time and space. *Sedimentary Geology*, **186**, (2006), 187-211.

Bossennec, C., Géraud, Y., Moretti, I., Mattioni, L., Stemmelen, D.: Pore network properties of sandstone in a fault damage zone. *Journal of Structural Geology*, **110**, (2018), 24-44.

Bucher, K., Stober, I.: Large-scale chemical stratification of fluids in the crust: hydraulic and chemical data from the geothermal site Urach, Germany. *Geofluids*, **16**, (2016), 813- 825.

Caine, J.S, Evans, J.P., Forster, C.B.: Fault zone architecture and permeability structure. *Geology*, **24**, (1996), 1025-1028.

Chester, F.M., Logan, J.M.: Composite planar fabric of gouge from the Punchbowl fault, California. *Journal of Structural Geology*, **9**, (1986), 621–634.

Childs, C., Manzocchi, T., Walsh, J.J., Bonson, C.G., Nicol, A., Schöpfer, M.P.P.: A geometric model of fault zone and fault rock thickness variations. *Journal of Structural Geology*, **31**, (2009), 117–127.

Cumming, W.B., Mackie, R.: 3D MT Resistivity Imaging for Geothermal Resource Assessment and Environmental Mitigation at the Glass Mountains KGRA, California. *GRC Transactions*, **31**, (2007), 331-334.

Cumming, W.B., Mackie, R.: Resistivity Imaging of Geothermal Resources Using 1D, 2D and 3D MT Inversion and TDEM Static Shift Correction Illustrated by a Glass Mountain Case History. *Proceedings*, World Geothermal Congress, Bali, Indonesia, (2010).

Davy, P., Darcel, C., Bour, O., Munier, R., de Dreuzy, J.R.: A note on the angular correction applied to fracture intensity profiles along drill core. *Journal of Geophysical Research*, **111**, (2006), B11408.

Dewes, T.J.B., Girardeau-Montaut, D., Allanic, C., Rohmer, J.: FACETS : a cloudcompare plugin to extract geological planes from unstructured 3D point clouds. *The International Archives of the Photogrammetry, Remote Sensing and Spatial Information Sciences*, Volume XLI-B5, 2016 XXIII ISPRS Congress, 12–19 July 2016, Prague, Czech Republic.

Edel, J.-B., Schulmann, K., Rotstein, Y.: The Variscan tectonic inheritance of the Upper Rhine Graben: evidence of reactivations in the Lias, Late Eocene–Oligocene up to the recent. *International Journal of Earth Science*, **96**, (2007), 305-325.

Edel, J.-B., Schulmann, K.: Geophysical constraints and model of the "Saxothuringian and Rhenohercynian subductions – magmatic arc system" in NE France and SW Germany. *Bulletin de la Société géologique de France*, **180**, (2009), 545-558.

Edel, J.-B., Maurer, V., Dalmais, E., Genter, A., Richard, A., Letourneau, O., Hehn, R.: Structure and nature of the Paleozoic basement based on magnetic, gravimetric and seismic inveestifations in the central Upper Rhinegraben. *Geothermal Energy*, **6**, (2018), 1-25.

Faulkner, D.R., Jackson, C.A.L., Lunn, R.J., Schlische, R.W., Shipton, Z.K., Wibberley, C.A.J., Withjack, M.O.: A review of recent developments concerning the structure, mechanics and fluid flow properties of fault zones. *Journal of Structural Geology*, **32**, (2010), 1557- 1575.

Faulkner, D.R., Mitchell, T.M., Jensen, E., Cembrano, J.: Scaling of fault damage zones with displacement and the implications for fault growth processes. *Journal of Geophysical Research*, **116**, (2011), B05403.

Faure, M., Monié, P., Pin, C., Maluski, H., Leloix, C.: Lat Visean thermal event in the northern part of the France Massif Central : new ^{40}Ar/39Ar and Rb-Sr isotopic constraints on the Hercynian syn-orogenic extension. *International Journal of Earth Sciences*, **91**, (2002), 53-75.

Faure, M., Lardeaux, J. M., Ledru, P.: A review of the pre-Permian geology of the Variscan French Massif Central. *Comptes-Rendus Geosciences*, **341**, (2009), 202–213.

Ferrill, D., Morris, A.: Dilational normal faults. *Journal of Structural Geology*, **25**, (2003), 183–196.

Ford, M., Le Carlier de Veslud, C., Bourgeois, O.: Kinematic and geometric analysis of fault-related folds in a rift setting: The Dannemarie basin, Upper Rhine Graben. *Journal of Structural Geology*, **29**, (2007), 1811-1830.

Forster, C.B., Evans, J.P.: Hydrogeology of thrust faults and crystalline thrust sheets: results of combined field and modeling studies. *Geophysical Research Letters*, **18**, (1991), 979–982.

Gray, M.B., Stamatakos, J.A., Ferrill, D.A., Evans, M.A.: Fault-zone deformation in welded tuffs at Yucca Mountain, Nevada, USA. *Journal of Structural Geology*, **27**, (2005), 1873– 1891.

Guillocheau, F., Robin, C., Allemand, P., Bourquin, S., Brault, N., Dromart, N., Friedenberg, R., Garcia, J.-P., Gaulier, J.-M., Gaumet, R., others: Meso-Cenozoic geodynamic evolution of the Paris basin: 3D stratigraphic constraints. *Geodynamica Acta*, **13**, (2000), 189–245.

Guy, A., Edel, J.B., Schulmann, K., Tomek, Č., Lexa, O.: A geophysical model of the Variscan orogenic root (Bohemian Massif): implications for modern collisional orogens. *Lithos*, **124**, (2011), 144–157.

Kim, Y.-S., Sanderson, D.J.: The relationship between displacement and length of faults: a review. *Earth-Scicnce Reviews*, **68**, (2005), 317-334.

Kushnir, A.R.L., Heap, M.J., Baud, P., Gilg, H.A., Reuschlé, T., Lerouge, C., Dezayes, C., Duringere, P.: Characterizing the physical properties of rocks from the Paleaozoic to Permo-Triassic transition in the Upper Rhine Graben. *Geothermal Energy*, **6**, (2018), 1-32.

Olivet, J.L.: Kinematics of the Iberian plate. *Bulletin des Centres de Recherches Exploration-Production Elf Aquitaine*, (1996), 131-195.

Lardeaux, J.M., Schulmann, K., Faure, M., Janoušek, V., Lexa, O., Skrzypek, E., Edel, J.B., Štípská, P.: The Moldanubian Zone in the French Massif Central, Vosges/Schwarzwald and Bohemian Massif revisited: differences and similarities. In: Schulmann, K., Martinez Catalan J.R., Lardeaux, J.M., Janoušek, V., Oggiano, G., The Variscan Orogeny: Extent, Timescale and the Formation of the European Crust. *Geological Society of London, Special Publications,* **405**, (2014), 7–44.

La Pointe, P., Parney, R., Eiben, T., Dunleavy, M., Whitney, J.: 3-D reservoir and stochastic fracture network modeling for enhanced oil recovery, circle ridge phosphoria/tensleep reservoir, wind river reservation, Arapaho and Shoshone tribes, Wyoming. Semi-Annual Technical Report, 75 p.

Le Garzic, E.: Distribution multi-échelle de la fracturation dans les réservoirs cristallins, influence de l'héritage structural. *Université de Strasbourg Phd thesis,* (2010), 268 p.

Le Maire, P., Bertrand, L., Munschy, M., Diraison, M., Géraud, Y.: Aerial magnetic mapping with an UAV and a fluxgate magnetometer: a new method for rapid mapping and upscaling from the field to regional scale. *Accepted in Geophysical Prospecting*.

Loveless, S.E., Bense, V.F., Turner, J.: Fault deformation processes and permeability architecture within recent rift sediments, central Greece. *Journal of Structural Geology*, **33**, (2011), 1554-1568.

Luthi, S.M.: Fractured reservoir analysis using modern geophysical well techniques: application to basement reservoirs in Vietnam. In : Harvey P.K., Brewer T.S., Pezard P.A., Petrov V.A., Petrophysical Properties of Crystalline Rocks. *Geological Society, London, Special Publications*, **240**, (2005), 95-106.

Matte, P.: The Variscan collage and orogeny (480±290 Ma) and the tectonic definition of the Armorica microplate: a review. *Terra Nova*, **13**, (2001), 122-128.

Massiot, C., Nicol, A., Townend, J., McNamara, D.D., Garcia-Sellés, D., Conway, C.E., Archibald, G.: Quantitative geometric description of fracture systems in an andesite lava flow using terrestrial laser scanner data. *Journal of Volcanology and Geothermal Research*, **341**, (2017), 315–331.

McCaffrey, K.J.W., Sleight, J.M., Pugliese, S., Holdsworth, R.E.: Fracture formation and evolution in crystalline rocks: insights from attribute analysis. In: Petford, N., McCaffrey, K.J.W. (Eds.), Hydrocarbons in Crystalline Rocks. *Geological Society, London, Special Publications*, **214**, (2003); 109-124.

Mitchell, T.M., Faulkner, D.R.: Towards quantifying the matrix permeability of fault damage zones in low porosity rocks. *Earth and Planetary Science Letters*, **339-340**, (2012), 24-31.

Mielke, P., Bär, K., Sass, I.: Determining the relationshop of thermal conductivity and compressional wave velocity of common rock types as a basis for reservoir characterization. *Journal of Applied Geophysics*, **140**, (2017), 135-144.

Nance, R.D., Gutiérrez-Alonso, G., Keppie, J.D., Linnemann, U., Murphy, J.B., Quesada, C., Strachan, R.A., Woodcock, N.H.: Evolution of the Rheic Ocean. *Gondwana Research*, **17**, (2010), 194–222.

Nelson, R.A.: Geologic Analysis of Naturally Fractured Reservoirs. 2nd edition, Boston, Gulf Professional Publishing, (2001), 332 p.

Riley, P.R., Goodwin, L.B., Lewis, C.J.: Controls on fault damage zone width, structure, and symmetry in the Bandelier Tuff, New Mexico. *Journal of Structural Geology*, **32**, (2010), 766–780.

Roussé, S., 2006. Architecture et dynamique des séries marines et continentales de l'Oligocène moyen et supérieur du Sud du Fossé Rhénan. Evolution des milieux de dépôt en contexte de rift en marge de l'avant-pays alpin. Université Louis Pasteur, Strasbourg, Phd thesis, 483 p.

Sausse, J., Dezayes, C., Dorbath, L., Genter, A., Place, J.: 3D model of fracture zones at Soultz-sous-Forêts based on geological data, image logs, induced microseismicity and vertical seismic profiles. *Comptes-Rendus Geoscience*, **342**, (2010), 531-545.

Sissingh, W.: Tectonostratigraphy of the West Alpine Foreland: correlation of Tertiary sedimentary sequences, changes in eustatic sea-level and stress regimes. *Tectonophysics*, **333**, (2010), 361–400.

Skrzypek, E., Schulmann, K., Tabaud, A.S., Edel, J.B., 2014. Palaeozoic evolution of the Variscan Vosges Mountains. In: Schulmann K., Martinez Catalan, J.R., Lardeaux, J.M., Janoušek, V., Oggiano, G. (eds) 2014. The Variscan Orogeny: Extent, Timescale and the Formation of the European Crust. *Geological Society, London, Special Publications*, **405**, (2014), 7–44.

Srivastava, S., Roest, W.R., Kovacs, L.C., Schouten, H., Kligord, K.: Iberian plate kinematics: A jumping plate boundary between Eurasia and Africa. *Nature*, **344**, (1990), 756-759.

Stober, I., Bucher, K.: Hydraulic properties of the crystalline basement. *Hydrogeology Journal*, **15**, (2007), 213-224.

Tabaud, A.S., Whitechurch, H., Rossi, P., Schulmann, K., Guerrot, C., Cocherie, A., 2014. Devonian-Permian magmatic pulses in the northern Vosges Mountains (NE France): result of continuous subduction of the Rhenohercynien Ocean and Avalonian passive margin. In: Schulmann K., Martinez Catalan, J.R., Lardeaux, J.M., Janoušek, V., Oggiano, G. (eds) 2014. The Variscan Orogeny: Extent, Timescale and the Formation of the European Crust. *Geological Society, London, Special Publications*, **405**, (2014), 7–44.

Walker, R.J., Holdsworth, R.E., Armitage, P.J., Faulkner, D.R.: Fault zone permeability structure evolution in basalts. *Geology*, **41**, (2013), 59–62.

Wang, X.: Stereological interpretation of rock fracture traces on borehole walls and other cylindrical surfaces. *Virginia Polytechnic Institute and State University Phd Thesis*, Blacksburg, (2005), 113 p.

Wilson, J.E., Goodwin, L.B., Lewis, C.J., 2003. Deformation bands in nonwelded ignimbrites: petrophysical controls on fault-zone deformation and evidence of preferential fluid flow. *Geology*, **31**, (2003), 837–840.